Physics Letters B 772 (2017) 403–408

Contents lists available at ScienceDirect

Physics Letters B

www.elsevier.com/locate/physletb

The impact of the intruder orbitals on the structure of neutron-rich Ag isotopes

Y.H. Kim [a,*], S. Biswas [b], M. Rejmund [a], A. Navin [a], A. Lemasson [a], S. Bhattacharyya [d], M. Caamaño [c], E. Clément [a], G. de France [a], B. Jacquot [a]

[a] GANIL, CEA/DRF - CNRS/IN2P3, Bd Henri Becquerel, BP 55027, F-14076 Caen Cedex 5, France
[b] DNAP, Tata Institute of Fundamental Research, Mumbai 400005, India
[c] USC, Universidad de Santiago de Compostela, E-15706 Santiago de Compostela, Spain
[d] Variable Energy Cyclotron Centre, 1/AF Bidhan Nagar, Kolkata 700064, India

ARTICLE INFO

Article history:
Received 7 March 2017
Received in revised form 6 June 2017
Accepted 20 June 2017
Available online 23 June 2017
Editor: V. Metag

Keywords:
Ag isotopes
Isotopic identification
Fission fragments
Large isospin and high angular momentum
Signature splitting and inversion
Shell-model

ABSTRACT

The low-lying high-spin yrast band structure of neutron-rich $^{113,118-121}$Ag has been established for the first time using prompt γ-ray spectroscopy of isotopically identified fission fragments produced in the ^{9}Be(^{238}U, $f\gamma$) fusion- and transfer-induced fission processes. The newly obtained level energies follow the systematics of the neighboring isotopes. The sequences of levels exhibit an energy inheritance from states in the corresponding Cd core. A striking constancy of a large signature splitting in odd-A Ag throughout the long chain of isotopes with $50 < N < 82$ and a signature inversion in even-A Ag isotopes, which are indications of triaxiality, were evidenced. These observed features were reproduced by large-scale shell-model calculations with a spherical basis for the first time in the Ag isotopic chain, revealing microscopically their complex nature with severely broken seniority ordering. The essential features of the observed signature splitting were further examined in the light of simplified, two-orbital shell-model calculations including only two intruder orbitals $\pi g_{9/2}$ and $\nu h_{11/2}$ from two consecutive shells above $Z = 50$ and $N = 82$ for protons and neutrons respectively, resulting in the $\pi g_{9/2}^{-3} \times \nu h_{11/2}^{m}$ configurations. The newly established bands were understood as fairly pure, built mainly on unique-parity intruder configurations and coupled to the basic states of the Cd core.

The collective and single-particle motion of the nucleons and their correlations can give rise to a variety of nuclear shapes, asymmetries, and excitation modes [1,2]. Triaxial nuclear shapes are directly manifested through the presence of various phenomena, like chirality and wobbling, and indirectly by signature splitting [1] and signature inversion. Gamma-ray spectroscopy is a major tool to experimentally explore the different facets of the above mentioned features [3]. Microscopic approaches of the shell model with a spherical basis (spherical shell model) are applied near shell closures while the deformed shell model (e.g. Nilsson model) with a deformed basis is used to describe mid-shell nuclei [4]. Large-scale shell-model calculations with a spherical basis can expand the calculable regions and can reproduce various aspects of nuclear structure from single-particle to collective motions [4] due to progress in computing power and associated techniques. However, there has been no attempt to account for the signatures of triaxiality in the framework of the spherical shell model in neutron-rich nuclei below Sn.

In neutron-rich nuclei below $Z = 50$, two intruder orbitals $\pi g_{9/2}$ and $\nu h_{11/2}$ lying near the Fermi surface are expected to play an important role. While going away from shell closures ($Z = 50$ and $N = 82$), the nucleon–nucleon correlations result in an increasing collectivity and associated deformations. In the case of axial deformation, the $\pi g_{9/2}$ orbital with a *high* angular momentum projection on the symmetry axis (Ω) and the $\nu h_{11/2}$ orbital with a *low* Ω, tend to drive the nucleus towards oblate and prolate deformation, respectively [5–7]. Hence, emergence of triaxial shapes is expected in this region, which can be associated with $\pi g_{9/2}^{n} \times \nu h_{11/2}^{m}$ configurations. Triaxial shapes have been shown to exist in neutron-rich isotopes near Ag (e.g. $^{112-118}$Rh [7,8] and $^{112-118}$Pd [9]) and the degree of triaxiality increases systematically in odd-Z isotopes, as one progresses from Y to Rh isotopes (Rh being in the vicinity of the $Z = 50$ shell closure) [2,10]. Esser et al. [11] established, using the systematics of the Pb region, that

* Corresponding author.
E-mail address: yunghee.kim@ganil.fr (Y.H. Kim).

http://dx.doi.org/10.1016/j.physletb.2017.06.058

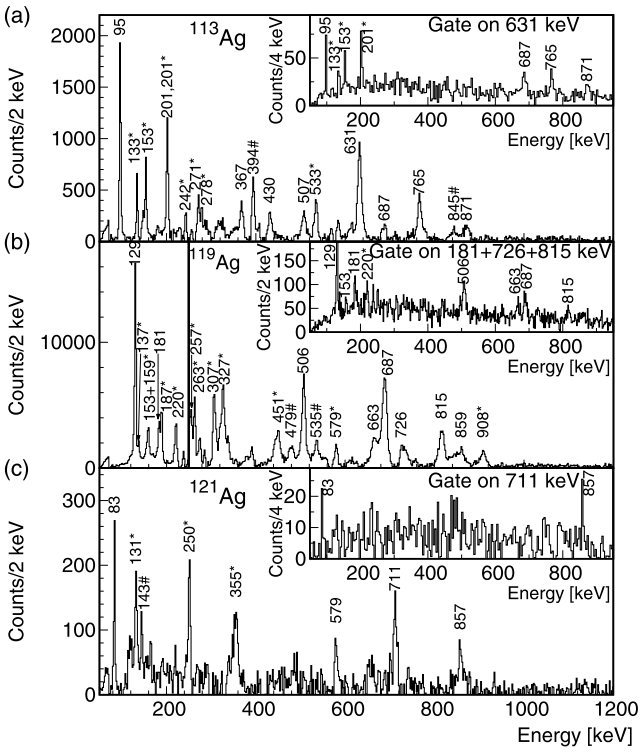

Fig. 1. The Doppler corrected γ-ray singles spectra for isotopically identified odd-A Ag isotopes (a) ^{113}Ag, (b) ^{119}Ag, and (c) ^{121}Ag. The ^{119}Ag singles spectrum is magnified by factor of 3 above 250 keV. γ–γ coincidence spectra are presented in the inset. Note that 201 keV in ^{113}Ag is a doublet (see text). The transitions assigned to side bands based on a coincidence between transitions are marked by (*). Transitions, not placed in the level scheme due to the lack of γ–γ coincidences, are marked by (#).

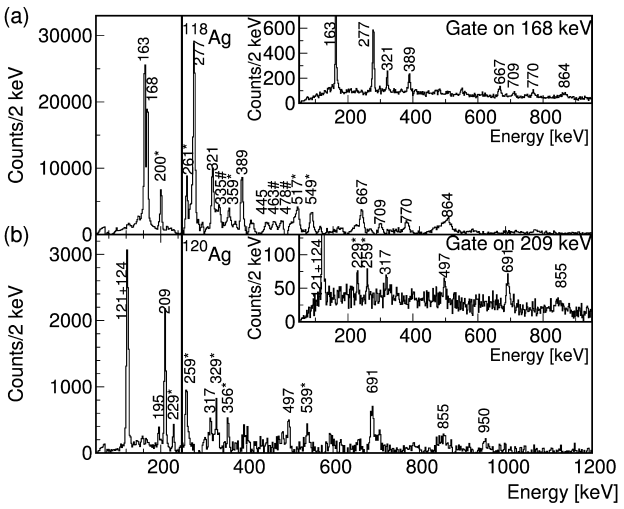

Fig. 2. The Doppler corrected γ-ray spectra for even-A Ag isotopes (a) ^{118}Ag and (b) ^{120}Ag. The singles spectra are magnified by 3 times above 250 keV. γ–γ coincidence spectra are shown in the inset. Note that the 121, 124 keV transitions are not resolved in (b) due to the 2 keV binning, but are resolved with a 1 keV/ch binning (see text). The labeling of the peaks is the same as in Fig. 1.

triaxiality reaches its maximum close to a shell closure and hence one could expect a large degree of triaxiality near Ag. Signatures of axial asymmetry have been established in the even-A Ag isotopes, i.e. γ-softness (^{106}Ag [12]), chirality (^{108}Ag [13]), and triaxial deformation (^{110}Ag [14]). In odd-A Ag isotopes chirality (^{107}Ag [15]) and triaxial deformation (^{109}Ag [14]) have been observed. For Ag isotopes with $A > 110$, the possibility of γ-softness in ^{115,117}Ag have been discussed [16]. Hence, the neutron-rich isotopes of Ag are an ideal region to explore nuclear structure properties related to triaxiality.

Theoretical interpretations for the region around the neutron-rich Ag isotopes were mainly carried out using deformed shell-model assuming a deformed core coupled to valence quasi-particles (e.g. triaxial rotor + particle model [7,17], tilted axis cranking model [18], triaxial projected shell-model [19], interacting boson model [20,21], and interacting boson–fermion plus broken pair model [22]). On the other hand, neutron-rich In and Cd isotopes were interpreted with the spherical shell model [23–26]. A microscopic view with the spherical shell model could bring a new perspective, e.g. the unexpected breaking of seniority (the number of unpaired nucleons) as observed in the neutron-rich In isotopes arising due to the proton–neutron interaction between the $\pi g_{9/2}$ and $\nu h_{11/2}$ orbitals [25]. The large dimensions associated with the relevant large-scale shell-model calculation limit its application in this region [26]. The $^{116-121}$Ag isotopes lie at the borderline of such large-scale shell-model calculations. In this letter, new experimental spectra for $^{113,118-121}$Ag are presented and compared to those of the neighboring nuclei. The experimentally observed features, including signature splitting and inversion, are analyzed using large-scale shell-model calculations with a spherical basis and a simplified, two-orbital shell-model approach.

The $^{113-121}$Ag isotopes were populated using transfer-fission and fusion–fission induced by a ^{238}U beam at 6.2 MeV/u (with a typical intensity of 0.2 pnA), impinging on a 10-micron thick ^{9}Be target [27]. The experiment was performed at GANIL using the VAMOS++ [28] spectrometer and the EXOGAM array [29]. The large-acceptance spectrometer VAMOS++, placed at 20° with respect to the beam axis, was used to isotopically identify the fission fragments. The detection system of the spectrometer was composed of (i) a pair of multi-wire parallel plate avalanche counters (MWPPAC) at target and focal plane (time-of-flight (ToF)), (ii) two drift chambers (x, y, θ_f, ϕ_f), (iii) an ionization chamber with segmented structure (ΔE), and (iv) 40 silicon detectors (E_r). A typical resolution in mass and atomic number was $\Delta A/A \sim 0.4\%$ and $\Delta Z/Z \sim 1.7\%$ [20,28], respectively. The prompt γ rays were detected using the EXOGAM array in coincidence with the isotopically identified fission fragments. EXOGAM consisted of 11 Compton-suppressed segmented clover HPGe detectors, placed 15 cm from the target. The Doppler correction of γ-ray energy was carried out using the velocity vector of the fragment and corresponding angle of the clover segment. Typical uncertainties of γ-ray energies were ~ 1 keV.

The newly observed level schemes of $^{113,118-121}$Ag were built based on the (i) coincidence between γ-ray transitions, (ii) relative intensities, and (iii) energy systematics of neighboring nuclides. The experimental setup is sensitive to the levels with lifetimes shorter than ~ 2 ns due to the geometry of the Compton shielding. This restricts the observed transitions to multi-polarities E1, M1, and E2, since higher-order transitions are unlikely. From the systematics of the neighboring isotopes, the γ-ray transitions between adjacent levels in the Ag isotopes were assigned as $\Delta J = 1$.

The isotopically identified and Doppler corrected γ-ray spectra for odd-A ^{113,119,121}Ag and even-A ^{118,120}Ag are shown in Figs. 1 and 2, respectively. The γ–γ coincidence spectrum for each isotope is shown in the inset. The transitions that could not be placed in the level scheme due to lack of γ–γ coincidences are indicated by (#) and transitions assigned to the side bands are marked by (*).

The level schemes of odd-A ^{113,119,121}Ag are presented in Fig. 3(a). The level scheme of ^{113}Ag was built on the 43.7 keV $7/2^+$ long-lived isomeric state [30] using the systematics of odd-A Ag isotopes. The γ–γ coincidence spectrum gated on the 533 keV transition (side band) shows peaks at 430 and 95 keV, therefore

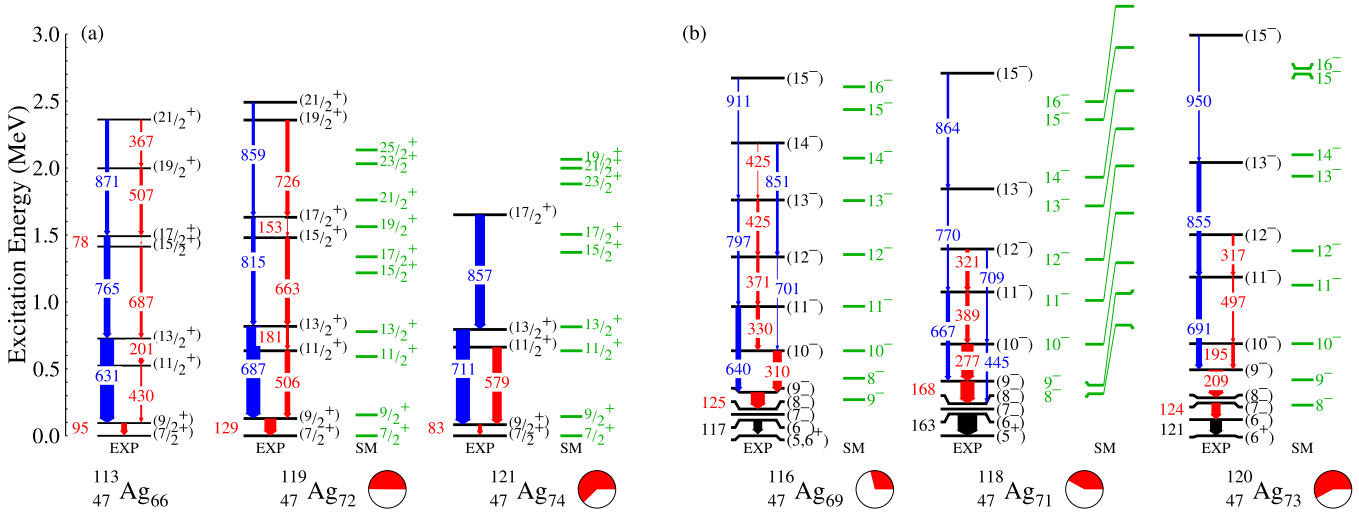

Fig. 3. (Color online.) Level diagram of the yrast bands of the measured Ag isotopes (a) odd-A (b) even-A indicated as EXP with corresponding yrast bands calculated by large-scale shell-model, indicated as SM. M1, E2, and E1 transitions are indicated as red, blue, and black arrows, respectively. The thickness of arrows represents the γ-ray intensity relative to the $(13/2^+) \rightarrow (9/2^+)$ or $(9^-) \rightarrow (8^-)$ transition for odd-A and even-A isotopes respectively. In the case of ^{118}Ag, a doublet yrare band calculated from the large-scale shell-model is also shown. The shell-model calculated levels for even-A isotopes are aligned to the (10^-) state for better display. The pie charts indicated in red are the calculated $\nu h_{11/2}$ occupancy (N) of $7/2^+$ and 8^- states for the odd-A and even-A Ag isotopes, respectively.

allowing us to place the 430 keV transition below the 201 keV transition. The 201 keV transition is a doublet since it remains very intense in the γ–γ coincidence spectrum gated on the 201 keV, and the second 201 keV transition belongs to the sideband. To determine the intensity of the 201 keV transition, the γ–γ coincidence spectrum gated on the 631 keV transition was used.

The ground states of ^{119,121}Ag were assigned as $J^\pi = (7/2^+)$ from β-decay measurements [31,32]. The lack of intensity was systematically observed for $(9/2^+) \rightarrow (7/2^+)$ transition for ^{113,119,121}Ag. The missing transition strength could be partially attributed to the internal conversion (IC) and the possible presence of a state with a lifetime of the order of 1 ns. For the 129 keV transition in ^{119}Ag, the IC coefficient is $\epsilon(\mathrm{M1}, 129\ \mathrm{keV}) = 0.206$ [33]. Using the γ–γ coincidence spectrum gated on the $663 + 815$ keV, and accounting for IC the ratio between transition strengths feeding/depopulating the $9/2^+$ state I(129 keV)/(I(687 keV) + I(506 keV)) is ~ 0.72. This reduced intensity of depopulating transitions could result from the in-flight decay from level with lifetime of the order of 1 ns. Same conclusions are valid for ^{113,121}Ag. Note that the present experimental setup was not appropriate for measurements of lifetimes of the order of 1 ns.

The level schemes of the newly observed even-A ^{118,120}Ag isotopes are presented in Fig. 3(b). The ^{118}Ag spectrum follows the systematics of the lighter Ag isotopes [17,34], where two intense transitions, 163 and 168 keV, were observed. There is an uncertainty on the ground state spin of ^{118}Ag being (2^-) [35] or (1^-) [36]. Following Ref. [35], the level scheme was built on the (5^+) long-lived (1.9 s) isomeric state at 127.6 keV decaying by an E3 transition to the ground state [35]. The two strong transitions of 163 and 168 keV were assigned as the two lowest transitions, $(9^-) \rightarrow (8^-)$ and $(6^-) \rightarrow (5^+)$ respectively, assuming two unknown transitions of $(8^-) \rightarrow (7^-)$ and $(7^-) \rightarrow (6^-)$ following the systematics [17,34]. In the coincidence spectrum gated on 277 keV, the relative intensity of 168 keV with respect to 163 keV transition (I(168 keV)/I(163 keV)) is ~ 0.98. Accounting for internal conversion ($\epsilon(\mathrm{M1}, 168\ \mathrm{keV}) = 0.100$ and $\epsilon(\mathrm{E1}, 163\ \mathrm{keV}) = 0.036$ [33]) the relative intensity is ~ 1.0. This indicates that the states in between (8^-, 7^- and 6^-) have lifetimes shorter than the order of 1 ns. This is different from the case of ^{116}Ag, where in the coincidence spectrum gated on the 310 keV transition the relative intensity of 117 keV peak with respect to the 125 keV peak (accounting for the corresponding IC coefficients) is ~ 0.82, indicating that the states, 8^-, 7^- and 6^-, decaying by M1 transitions could have lifetimes of the order of 1 ns.

In ^{120}Ag, the tentative level scheme was built on the long-lived isomeric state of ^{120}Ag (0.32 s), which was determined to be $J = 6$ [37], and assuming a positive parity. Three intense γ-ray transitions of 121, 124, and 209 keV were observed. In the spectrum with 1 keV binning and the corresponding γ–γ coincidence spectrum gated on the 209 keV transition, the 121 and 124 keV transitions are clearly separated. The 121 keV peak is seen in the coincidence spectra gated on 356 and 539 keV transitions (from the side band), bypassing the 124 and 209 keV transition. This allows us to place the 121 keV transition as the depopulating transition from the lowest excited state. In the γ–γ coincidence spectrum gated on the 209 keV transition, the intensity of the 124 keV peak relative to the 121 keV peak is ~ 0.92. Accounting for IC coefficient ($\epsilon(\mathrm{M1}, 124\ \mathrm{keV}) = 0.230$ and $\epsilon(\mathrm{E1}, 121\ \mathrm{keV}) = 0.093$ [33]) the relative intensity becomes ~ 0.97. This indicates that the 7^- and 6^- states have lifetime shorter than 1 ns. However, from the γ–γ coincidence spectrum gated on the 691 keV transition, the transition strength of the 124 keV peak relative to the 209 keV peak (corrected for IC coefficient) is I(124 keV)/I(209 keV) ~ 0.75, which could indicate that a possible lifetime of the order of 1 ns of the 8^- state. Therefore, we assumed an unobserved transition between (8^-) and (7^-) states, and placed the 124 keV peak as $(7^-) \rightarrow (6^-)$ transition. Note that the unobserved transition is introduced in the ^{118,120}Ag level scheme to match the systematics from light Ag isotope and build the level schemes connected to already observed states from the previous β/isomer-decay experiments. The presence and placement of the unobserved transitions is tentative.

The newly established level schemes of odd-A ^{113,119,121}Ag isotopes smoothly follow the systematics of odd-A Ag isotopes, persisting throughout $50 < N < 82$ [38]. The energies of $7/2^+$, $11/2^+$, and $15/2^+$ levels follow closely the 0^+, 2^+, and 4^+ levels in even-A Cd isotopes, respectively (see Ref. [38]). This is illustrated in Fig. 4(a). The coinciding level energies strongly indicate a structural relationship (inheritance) between states in Ag and those in the corresponding Cd core. This points towards the following

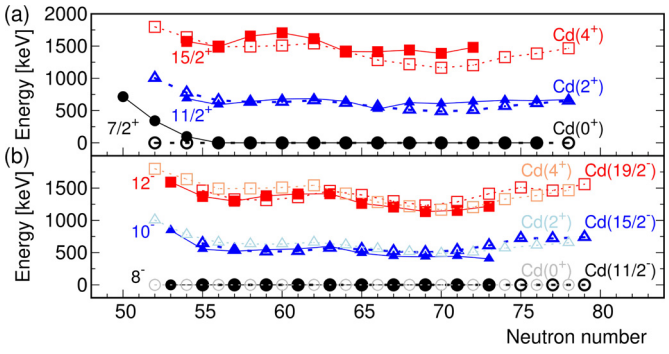

Fig. 4. (Color online.) Evolution of level energies of Ag isotopes and the corresponding Cd core coupled states. (a) Odd-A Ag $7/2^+$, $11/2^+$, and $15/2^+$ states with even-A Cd 0^+, 2^+, and 4^+ states. (b) Even-A Ag 8^-, 10^-, and 12^- with odd-A Cd ($11/2^-$, $15/2^-$, and $19/2^-$ states) and even-A Cd (0^+, 2^+, and 4^+ states). The energies of the levels of Ag isotopes are shown with filled symbols and those of Cd isotopes are presented with open symbols. For the even-A Ag and odd-A Cd levels, the excitation energy of the 8^- and $11/2^-$ state of the corresponding isotope was respectively subtracted.

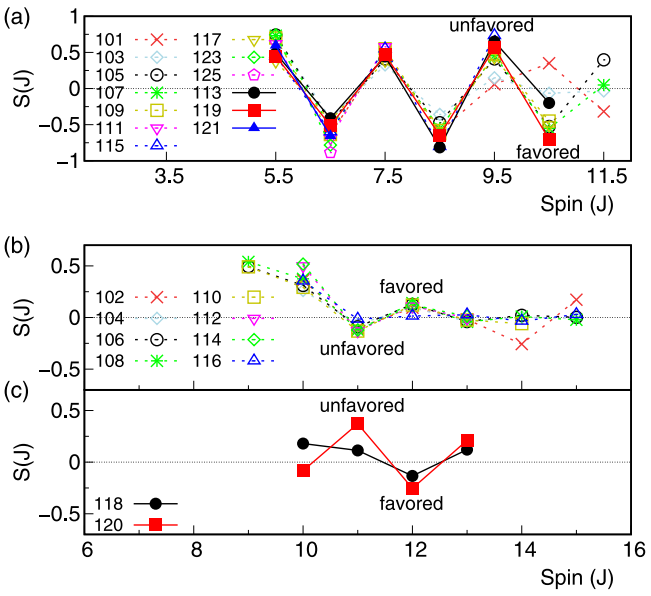

Fig. 5. (Color online.) Signature splitting for the yrast band of Ag isotopes (a) odd-A $^{101-125}$Ag, even-A (b) $^{102-116}$Ag (signature inversed), and (c) $^{118-120}$Ag (normal signature splitting). The new experimental data from this work in $^{113,118-121}$Ag are indicated as filled points and solid line. The unfavored and favored signatures are stated in the figure. The dotted line indicating $S(J) = 0$ is shown to guide the eye.

understanding of their structure, $7/2^+_\pi \times \mathrm{Cd}(0^+)$, $7/2^+_\pi \times \mathrm{Cd}(2^+)$, and $7/2^+_\pi \times \mathrm{Cd}(4^+)$, respectively. The $7/2^+$ ground state results from a configuration with seniority $\nu = 3$ for three proton configuration $(\pi g^{-3}_{9/2})$ [38]. It is different from the case of In, where the Sn core coupled states are built on a $9/2^+$ state $(\pi g^{-1}_{9/2})$ [23,24]. A large energy staggering of adjacent M1 transitions favors the development of a more intense E2 decay branch when the M1 energy is small ($13/2^+$, $17/2^+$, and $21/2^+$). In the opposite case, E2 transitions are hindered. Similarly, the negative parity levels of even-A Ag isotopes smoothly follow the systematics of the lighter isotopes. The energies of the 8^-, 10^-, and 12^- states follow those of the corresponding $11/2^-$, $15/2^-$, and $19/2^-$ states in odd-A Cd isotopes. Note that neither $11/2^-$ in Cd nor 8^- in Ag are the ground states, therefore in Fig. 4(b) their excitation energies have been subtracted. A similar inheritance relationship is evident from Fig. 4(b) and thus one could describe the 8^-, 10^- and 12^- states in even-A Ag as $7/2^+_\pi \times \mathrm{Cd}(11/2^-)$, $7/2^+_\pi \times \mathrm{Cd}(15/2^-)$, and $7/2^+_\pi \times \mathrm{Cd}(19/2^-)$, or as $8^- \times \mathrm{Cd}(0^+)$, $8^- \times \mathrm{Cd}(2^+)$, and $8^- \times \mathrm{Cd}(4^+)$, respectively.

The signature splitting $S(J)$ [39,40] is often used as observable evidence of triaxiality (in particular its large amplitude [7,10]). The $S(J)$ is defined as

$$S(J) = \frac{E(J) - E(J-1)}{E(J) - E(J-2)} \frac{J(J+1) - (J-2)(J-1)}{J(J+1) - J(J-1)}$$

where J is the spin of the state and $E(J)$ is the corresponding excitation energy. The favored signature has a lower value of $S(J)$ than the unfavored signature, with exceptions in the case of signature inversion (or anomalous signature splitting). The plausible origins of signature inversion are triaxiality [22,41,42], proton–neutron interaction [43,44], or both [45–47]. The signature splitting $S(J)$ of odd-A and even-A Ag isotopes is presented in Fig. 5. A large-amplitude signature splitting is observed in odd-A Ag isotopes (two times larger than that for neighboring Rh isotopes [8]). As evident from Fig. 5(a), the magnitude of $S(J)$ for the newly observed ^{113,119,121}Ag is similar to that in $^{101-125}$Ag [48]. In even-A Ag isotopes, a signature inversion occurs at low-lying states for $^{102-116}$Ag [48] with similar amplitudes (Fig. 5(b)) and changes to the normal signature for ^{118,120}Ag (Fig. 5(c)). Similarly, signature inversion was observed in even-A Rh isotopes at $N \leq 69$ [7], while In isotopes do not show such a feature. The constancy in the amplitude of signature splitting throughout a long chain of Ag isotopes for both odd-A and even-A is striking. The following questions arise, from the observed signature splitting in Ag: (i) what is the origin of the constant amplitude in signature splitting? and (ii) what is the underlying reason for the sudden change of signature from inversed to normal in even-A isotopes between ^{116,118}Ag?

Large-scale shell-model calculations were carried out with a restricted model space from the *jj45pna* interaction consisting of orbitals near the Fermi level (proton $g_{9/2}$, $p_{1/2}$ and neutron $d_{3/2}$, $s_{1/2}$, $h_{11/2}$) following the same method as in Ref. [25]. This allowed the calculation of $^{116-121}$Ag levels with $J \geq 7/2^+$ (odd-A) and $J \geq 8^-$ (even-A). The shell-model calculations reproduce the experimental level ordering in both odd-A and even-A Ag isotopes except for the 8^- and 9^- states in ^{116}Ag (Fig. 3(b)), which is at the limit of applicability of the model. The level ordering in ^{123,125}Ag [38] is also reproduced by the calculations (not shown). It should be noted that in the calculation using the full *jj45pna* model space, the level ordering and the energies were not reproduced at all [38,49]. In our work, the calculated energy levels appear compressed as a function of decreasing neutron number, compared to the experimental data. Similarly, the calculated spectra of even–even Cd isotopes are compressed (not shown). It could possibly be related to the restricted model space resulting in an insufficient degree of collectivity [38], although the corresponding signature splitting is in good agreement with the experimental data (Fig. 6). The transition from the inverted signature in ^{116}Ag to the normal signature in ^{118,120}Ag is also reproduced. The calculated wave functions of states in the Ag isotopes, while dominated by the $\pi g^{-3}_{9/2} \times \nu h^m_{11/2}$ configurations, are strongly mixed and composed of different proton and neutron excitations. Therefore, it is difficult to single out the corresponding inheritance of the core coupled state from their wave functions. The wave functions of states in underlying even–even Cd ground states as well as the excited states are already very strongly mixed. For example, for ^{120}Cd the 0^+ ground state is mainly composed of $\sim 40\%(0^+_\pi \times 0^+_\nu) + \sim 35\%(2^+_\pi \times 2^+_\nu)$ excitations and the first 2^+ state of $\sim 35\%(0^+_\pi \times 2^+_\nu) + \sim 24\%(2^+_\pi \times 0^+_\nu) + \sim 16\%(2^+_\pi \times 2^+_\nu)$ excitations. However, the energy inheritance relation between Ag and Cd as deduced from Fig. 4 is reproduced in the calculation.

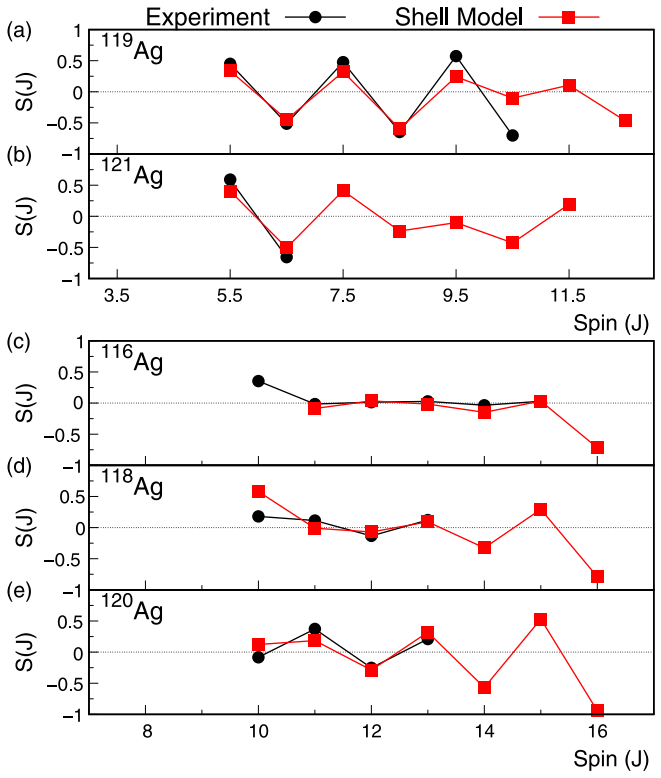

Fig. 6. (Color online.) Signature splitting of the measured yrast band of Ag isotopes and the corresponding large-scale shell-model calculation results in odd-A (a) ^{119}Ag and (b) ^{121}Ag, even-A (c) ^{116}Ag, (d) ^{118}Ag, and (e) ^{120}Ag. The ^{121}Ag shell-model calculation followed the yrare band at $J \geq 17/2^{+}$.

Since the large-scale shell-model calculations suggest that the structure of Ag isotopes is mostly determined by the $\pi g_{9/2}^{-3} \times \nu h_{11/2}^{m}$ configuration, a simplified two-orbital shell-model calculation, with a configuration space consisting only of $\pi g_{9/2}$ and $\nu h_{11/2}$ orbitals was carried out for deeper understanding of the experimental observations. The level energies are reasonably reproduced given the simplicity of the model. In Fig. 7(a), the calculated signature splitting for odd-A Ag isotope is shown as a function of the $\nu h_{11/2}$ occupancy ($N_{h_{11/2}}$). The large amplitude of the signature splitting and its constancy for different $N_{h_{11/2}}$ is reproduced. The wave functions of states with favored signature (e.g. $13/2^{+}$, $17/2^{+}\ldots$) show a similar proton–neutron coupling ($|J\rangle = |J_{\pi} \times J_{\nu}; J\rangle$) to the unfavored $|J-1\rangle$ below. The average summed proton–neutron seniority $\langle v_{\pi\nu}\rangle$ ($v_{\pi\nu} = v_{\pi} + v_{\nu}$) of favored $|J\rangle$ is similar relative to the unfavored $|J-1\rangle$ (e.g. $11/2^{+}$, $15/2^{+}\ldots$) state below. On the other hand, the unfavored $|J+1\rangle$ state above the $|J\rangle$ state has a different proton–neutron coupling and larger average seniority compared to the $|J\rangle$ state. Therefore, an extra energy is needed relative to the $|J\rangle$ state which could induce signature splitting. Fig. 7(b) and (c) show the calculated signature splitting for even-A isotopes. The signature inversion is reproduced at the occupancy $N_{h_{11/2}} \leq 3$; the amplitude becomes minimum at $N_{h_{11/2}} = 5$ and evolves to normal signature with a similar amplitude at $N_{h_{11/2}} \geq 7$. The transition from inverted to the normal signature splitting corresponds to the transition from the hole–particle to the hole–hole configuration in the $\pi g_{9/2}^{-3} \times \nu h_{11/2}^{m}$ multiplet. The $\nu h_{11/2}$ occupancy, where the signature inversion changes to the normal signature splitting, corresponds to that of ^{116}Ag and ^{118}Ag. The wave functions of proton–neutron coupled states evolve smoothly with spin regardless of favored/unfavored signature, resulting in a relatively small signature splitting. The calculated wave functions are further analyzed in terms of the

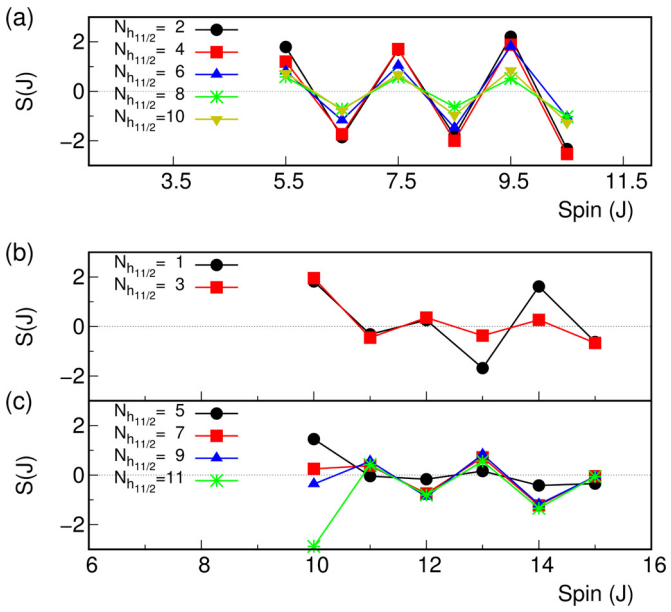

Fig. 7. (Color online.) Signature splitting calculated using the simplified two-orbital shell-model calculation as a function of $\nu h_{11/2}$ occupancy ($N_{h_{11/2}}$) for (a) odd-A, even-A (b) $N_{h_{11/2}} \leq 3$, and (c) $N_{h_{11/2}} \geq 5$ Ag isotopes.

summed proton–neutron seniority ($v_{\pi\nu}$). In the case of odd-A Ag isotopes, the $v_{\pi\nu} = 3$ component (1 broken pair) dominates for the $7/2^{+}$ state, where the probability of a proton pair breaking is greater than that of neutrons. For the $9/2^{+}$ state the $v_{\pi\nu} = 1$ component (0 broken pairs) dominates, except for $6 \leq N_{h_{11/2}} \leq 8$, where $v_{\pi\nu} > 3$ dominates. For the 8^{-} states in even-A Ag, seniority $v_{\pi\nu} = 2$ (0 broken pairs) dominates when $\nu h_{11/2}$ is either almost full or empty; in between it evolves, i.e. $4 \leq v_{\pi\nu} \leq 6$ for $5 \leq N_{h_{11/2}} \leq 9$. For the 9^{-} states, seniority evolves from $v_{\pi\nu} = 2$ to $v_{\pi\nu} = 4$ as the $\nu h_{11/2}$ occupancy increases. In general, the breaking of the natural seniority ordering in Ag isotopes occurs at a lower particle/hole occupation in the $\nu h_{11/2}$ orbital over a wide range of spin (J) and average seniority ($\langle v_{\pi\nu}\rangle$) is larger as compared to the In isotopes [25].

The new experimental features revealed in this work over a long range of isotopes, i.e., the characteristic signature splitting for the odd-A and even-A Ag, can be reproduced using the simplified, two-orbital shell-model approach. This indicates that the structure of the yrast band in the Ag isotopes can be essentially understood based on $\pi g_{9/2}^{-3} \times \nu h_{11/2}^{m}$ configurations using a realistic nucleon–nucleon interaction, without any particular assumption about the deformation of the nuclei. The strong mixing in the wave functions, which is also present in the Cd core, originates from the competition between pairing of like-nucleons and the proton–neutron interaction, creating large breaking of the natural seniority ordering [25]. Further, the extended large-scale shell-model calculation results in increased collectivity and reproduces the band structure in finer detail. The observed simplicity behind the complex structures in the wave functions could be due to the strong contribution of both proton and neutron intruder orbitals with unique parity, which makes the configuration of the band fairly pure.

In summary, the excited states of neutron-rich $^{113,118-121}$Ag were observed for the first time using prompt γ-ray spectroscopy of isotopically identified fission fragments. The evolution of level energies in both even-A and odd-A Ag isotopes follows the systematics between $50 < N < 82$, exhibiting a clear inheritance from the Cd core. The Ag isotopes present large signature splitting in odd-A and inverted signature in even-A. Both signatures are usu-

ally regarded as evidence of triaxiality. A striking constancy of signature splitting over a wide range of Ag isotopes was observed. Large-scale shell-model calculations were performed for $^{116-121}$Ag, which reproduce the ordering and energy of the experimental levels for the first time in this region. These calculations, without any assumption on the deformation, reproduce the features of experimental signature splitting. The large-scale shell-model calculations do not provide a direct information about the shape of the nucleus, thus the shell model does not provide the direct evidence of the presence of the triaxial deformation. Further, the model predicts a yrare band with similar energy spacing as the yrast band in ^{118}Ag (Fig. 3(b)). The experimental observation of such a band is often interpreted as evidence for chirality and its prediction by the spherical shell model is striking. A further simplified, two-orbital shell-model calculation, considering only the $\pi g_{9/2}^{-3} \times \nu h_{11/2}^{m}$ configurations reproduces the essential features of signature splitting, which could be interpreted as due to the $\nu h_{11/2}$ occupancy. The natural seniority ordering for both neutrons and protons was found to be more strongly broken in Ag isotopes than in In isotopes.

The successful model description of different features related to the signature splitting shown in this work represents a very promising step towards a unified view of nuclear structure [4]. Large-scale shell-model calculations, using a complete proton and neutron configuration space, for nuclei close to neutron mid-shell would be of great interest. First, they could provide the complete microscopic and assumption-free insight into the characteristic structures arising from triaxiality like chirality or wobbling. Second, they could provide a link and a point of convergence with deformed shell models. Experimentally, the extension to higher spins in more neutron-rich isotopes of Ag or the observation of predicted yrare, doublet bands can be carried out with the next generation γ-ray tracking detectors with higher sensitivity.

Acknowledgements

We would like to thank C. Schmitt, F. Farget, and O. Delaune for help in various aspects of data collection and the analysis and P. Van Isacker for useful discussions and a critical reading of the manuscript. We acknowledge the important technical contributions of J. Goupil, G. Fermont, L. Ménager, J. Ropert, C. Spitaels, and the GANIL accelerator staff. S. B., and S. B. acknowledge partial financial support through the LIA France-India agreement.

References

[1] S. Frauendorf, Rev. Mod. Phys. 73 (2001) 463.
[2] P. Möller, et al., At. Data Nucl. Data Tables 98 (2012) 149.
[3] M.A. Riley, J. Simpson, E.S. Paul, Phys. Scr. 91 (2016) 123002.
[4] E. Caurier, et al., Rev. Mod. Phys. 77 (2005) 427.
[5] X.Q. Zhang, et al., Phys. Rev. C 61 (1999) 014305.
[6] Y.X. Luo, et al., Phys. Rev. C 69 (2004) 024315.
[7] S.H. Liu, et al., Phys. Rev. C 83 (2011) 064310.
[8] A. Navin, et al., Phys. Lett. B 767 (2017) 480–484.
[9] Y. Luo, et al., Nucl. Phys. A 919 (2013) 67.
[10] Y.X. Luo, et al., J. Phys. G 31 (2005) 1303.
[11] L. Esser, et al., Phys. Rev. C 55 (1997) 206.
[12] P. Joshi, et al., Phys. Rev. Lett. 98 (2007) 102501.
[13] J. Sethi, et al., Phys. Lett. B 725 (2013) 85.
[14] S. Roy, et al., Phys. Lett. B 710 (2012) 587.
[15] B. Qi, et al., Phys. Rev. C 88 (2013) 027302.
[16] J.K. Hwang, et al., Phys. Rev. C 65 (2002) 054314.
[17] M.-G. Porquet, et al., Eur. Phys. J. A 15 (2002) 463.
[18] Y. Luo, et al., Nucl. Phys. A 874 (2012) 32.
[19] G. Bhat, et al., Phys. Lett. B 738 (2014) 218.
[20] A. Navin, et al., Phys. Lett. B 728 (2014) 136.
[21] B. Sorgunlu, P. Van Isacker, Nucl. Phys. A 808 (2008) 27.
[22] J. Timár, et al., Nucl. Phys. A 696 (2001) 241.
[23] J. Van Maldeghem, K. Heyde, J. Sau, Phys. Rev. C 32 (1985) 1067.
[24] M.-G. Porquet, et al., Eur. Phys. J. A 20 (2004) 245.
[25] M. Rejmund, et al., Phys. Lett. B 753 (2016) 86.
[26] M. Rejmund, et al., Phys. Rev. C 93 (2016) 024312.
[27] A. Navin, R. Maurycy, Gamma-ray spectroscopy of neutron-rich fission fragments, in: AccessScience, McGraw-Hill Education, 2014.
[28] M. Rejmund, et al., Nucl. Instrum. Methods Phys. Res., Sect. A, Accel. Spectrom. Detect. Assoc. Equip. 646 (2011) 184.
[29] J. Simpson, et al., Acta Phys. Hung. A, Heavy Ion Phys. 11 (2000) 159.
[30] J. Rogowski, et al., Phys. Rev. C 42 (1990) 2733.
[31] B. Fogelberg, P. Hoff, Nucl. Phys. A 391 (1982) 445.
[32] H. Penttilä, et al., Z. Phys. A 338 (1991) 291.
[33] T. Kibédi, et al., Nucl. Instrum. Methods Phys. Res., Sect. A, Accel. Spectrom. Detect. Assoc. Equip. 589 (2008) 202.
[34] M.-G. Porquet, et al., Eur. Phys. J. A 18 (2003) 25.
[35] Z. Janas, et al., Nucl. Phys. A 552 (1993) 340.
[36] B. Fogelberg, A. Bäcklin, T. Nagarajan, Phys. Lett. B 36 (1971) 334.
[37] J. Rissanen, et al., Eur. Phys. J. A 34 (2007) 113.
[38] S. Lalkovski, et al., Phys. Rev. C 87 (2013) 034308.
[39] N. Zamfir, R. Casten, Phys. Lett. B 260 (1991) 265.
[40] A. Gelberg, et al., Nucl. Phys. A 557 (1993) 439.
[41] I. Hamamoto, B. Mottelson, Phys. Lett. B 127 (1983) 281.
[42] R. Bengtsson, et al., Nucl. Phys. A 415 (1984) 189.
[43] I. Hamamoto, Phys. Lett. B 235 (1990) 221.
[44] L. Riedinger, et al., Prog. Part. Nucl. Phys. 38 (1997) 251.
[45] N. Tajima, Nucl. Phys. A 520 (1990) c317.
[46] N. Tajima, Nucl. Phys. A 572 (1994) 365.
[47] Z.-C. Gao, Y. Chen, Y. Sun, Phys. Lett. B 634 (2006) 195.
[48] ENSDF, http://www.nndc.bnl.gov/ensdf/, 2017.
[49] I. Stefanescu, et al., Eur. Phys. J. A 42 (2009) 407.